Journal of Molecular Modeling (2022) 28: 76
https://doi.org/10.1007/s00894-022-05073-3

ORIGINAL PAPER

Three new inhibitors of class A β-lactamases evaluated by molecular docking and dynamics simulations methods: relebactam, enmetazobactam, and QPX7728

Ayşegül Saral Sariyer[1]

Received: 1 September 2021 / Accepted: 26 February 2022 / Published online: 4 March 2022
© The Author(s), under exclusive licence to Springer-Verlag GmbH Germany, part of Springer Nature 2022

Abstract
Antibiotic-resistant *Acinetobacter baumannii*, *Pseudomonas aeruginosa*, *Mycobacterium tuberculosis*, *Staphylococcus aureus*, and *Enterobacterales* infections are serious global health problems, and class A β-lactamases are one mechanism that leads to antibiotic resistance. QPX7728, relebactam, and enmetazobactam are new β-lactamase inhibitors to combat β-lactam resistance. in silico approach was used in the current study to find which of the three inhibitors would be more effective for all class A β-lactamases and to reveal molecular insights into the differences between their binding energies. The mutations in conserved residues of the active sites of β-lactamases were defined using BLDB and Clustal Omega. FastME and MMseq2 were used for cluster and phylogeny analysis. 3D protein structure models for β-lactamases were built using SWISS-MODEL. ERRAT and Galaxy Web Server were used to verify 42 β-lactamase protein structures. QPX7728, relebactam, and enmetazobactam were docked to β-lactamases by using AutoDock 4.2. The TEM76-relebactam, CTX-M-81-relebactam, TEM-76-enmetazobactam, and CTX-M-200-enmetazobactam complexes were simulated by molecular dynamics method for 500 ns. Based on molecular docking results, relebactam and QPX7728 were more favorable inhibitors for serine A β-lactamases. A 2D representation of the interactions between ligands and β-lactamases showed that S235, hydrogen bonded with TEM-76, might play a role in inhibitor design. A 500-ns MD analysis of complexes indicated that distance from S70, stability in the enzyme active cavity, and high atomic displacement would account for a significant difference in inhibitor binding affinity.

Keywords Relebactam · Enmetazobactam · QPX7728 · Class A β-lactamases · Molecular docking · Molecular dynamic simulations

Introduction

For years, β-lactams have been the safest and most prescribed group of antibiotics for the treatment of treating infections caused by bacteria. Penicillin, cefpodoxime, cefuroxime axetil, cefepime, ertapenem, imipenem, and meropenem are some examples of antibiotics in this group [1]. With the clinical use of these antibiotics, a new and incessant global public health problem has emerged: antibiotic resistance. One of the mechanisms leading to β-lactam resistance is the enzymatic degradation of this group of antibiotics by β-lactamases. The β-lactamases are divided into four structural groups class A, B, C, and D according to their amino acid similarities [2]. Class A serine β-lactamases inactivate β-lactams through an acylation-deacylation reaction triggered by nucleophilic attack of the active series, in which Glu166 acts as the activating base [3]. Antibiotic-resistant *Acinetobacter baumannii*, *Pseudomonas aeruginosa*, *Mycobacterium tuberculosis*, *Staphylococcus aureus*, and *Enterobacterales* were listed in the 2019 AR Threats Report. This report sounded the alarm to the danger of infections caused by these bacteria (https://www.cdc.gov/drugresistance/biggest-threats.html). One of the mechanisms that cause antibiotic resistance in these bacteria is class A β-lactamases. Class A β-lactamases are divided into subclasses A1 and A2 based on conserved motifs S70XXK, S130DN, K234TG, catalytic base E166, and amino acid residues G45, F66, V80, L81, L91, L101, P107, A134, L138, G143, G144, G156, L169,

✉ Ayşegül Saral Sariyer
asaral@artvin.edu.tr

[1] Department of Nutrition and Dietetics, Faculty of Health Sciences, 08000 Artvin, Turkey

T181, T182, and P183 (Ambler numbering) [4]. CfxA, CepA, CblA-1, VEB-1, CSP-1, CIA-1, TLA-1, and PER-1 belonged to subclassA2 and other class A β-lactamases are belonged to subclass A1, e.g., IMI-1, CTX-M-1, TEM-1, and SHV-1 [5].

β-Lactamase inhibitors have been discovered to potentiate existing antibiotics to combat β-lactam resistance. The first of these was clavulanic acid, and later tazobactam and sulbactam were discovered as class A β-lactamase inhibitors. These inhibitors are suicide inhibitors that permanently inactivate the enzyme through secondary chemical reactions at the active site [6] Although the combination of these inhibitors with β-lactams has been used in the treatment of various infections, the rapid evolution of β-lactamases into new alleles has led to the discovery of broad-spectrum inhibitor candidates. Three compounds from which these new inhibitor candidates are derived: diazabicyclooctanones, boronate-based compounds, and β-lactam compounds [7]. Relebactam, avibactam, zidebactam, durlobactam, nacubactam, ETX1317, and WCK 4234 were diazabicyclooctane serine β-lactamase inhibitors and relebactam has been approved for treatment of complicated urinary tract infections and complicated intraabdominal infections [8, 9]. Vaborbactam, taniborbactam, VNRX-5236, and QPX7728 which are boronate-based inhibitors with tetrahedral form are an analog of intermediates of acylation-deacylation reaction, and they are of mechanistically important for the inhibition of serine and metallo-β-lactamases [9, 10]. QPX7728 is a new boronate derivative inhibitor that can inhibit class A, B, and D carbapenemases such as KPC, NDM, VIM, OXA-48, and OXA-23 [11]. Enmetazobactam is a β-lactam–derived inhibitor with a methyl group in the triazole moiety, which is thought to increase interactions with β-lactamases, and its combination with cefepime has been found to reduce bacterial growth in cefepime-resistant *Enterobacteriacea* [12]. Serine beta-lactamase inhibitors have same binding site with beta-lactams [13]. In the study investigating the molecular basis of class A β-lactamase relebactam inhibition mechanism, it was observed that the inhibitor is positioned to form hydrogen bonds with the oxyanion hole (S70 and T237 backbone amides), N132, and S130 [14]. The crystal structure of KPC-2 with QPX7728 indicates that the inhibitor is located at the active site of the enzyme [15].

The molecular docking approach is used to model the interaction between a ligand and a protein at the atomic level [16]. Molecular dynamics (MD) simulations predict how each atom in a protein will move over time and reveal the positions of all atoms. It can also predict how biomolecules will respond at the atomic level if a ligand is added [17]. These in silico approaches have been used to predict versatile inhibitors for β-lactamases.

in silico approach was used in the current study to find which of the three inhibitors would be more effective for all class A β-lactamases and to reveal molecular insights into the differences between their binding energies. The results of this study may reveal information that can be used as preliminary data in the design of new inhibitors. The parameters which were used to determine enzymes (Supplementary file, Table S1); among all subclasses, A1 and A2 class A β-lactamases were as follows: (i) β-lactamases detected in bacteria listed in 2019 AR Threats Report and (ii) β-lactamases with mutations in their active sites (T237, T235, S70, K234, S130, K73, and W105). Relebactam, enmetazobactam, and QPX7728 were selected as inhibitors. There are three factors that go into choosing relebactam, enmetazobactam, and QPX7728: (i) choosing new inhibitors from diazabicyclooctanones, boronate-based compounds and β-lactam–derived compounds, (ii) relebactam is effective in reversing imipenem resistance, (iii) enmetazobactam is the only β-lactam–derived class A β-lactamase inhibitor, (iv) QPX7728 is the last derived inhibitor with its ultra spectrum.

Materials and methods

Detection of mutations in conserved residues of class A β-lactamase active site

Amino acid residues in the active site are T237, T235, S70, K234, S130, K73, and W105 in β-lactamases. Substitutions in these amino acid residues were determined by using BLDB (B-Lactamase Database-Structure and Function) and Clustal Omega [18]. Amino acid substitutions were checked for all class A serine β-lactamases which were found in bacteria listed in the 2019 AR Threats Report (Supplementary file Table S1). Besides, amino acid substitutions were determined both in different types of β-lactamase and among their alleles. It was found by MMseq2 that selected 42 class A serine β-lactamases were divided into 22 clusters [19]. FastME web-based tool [20] and iTOL v6 (https://itol.embl.de/) were used for phylogeny analysis and management of phylogenetic tree, respectively.

3D Protein structure modeling

3D protein structure models of 32 β-lactamases were built using the SWISS-MODEL homology-modeling pipeline [21]. However, PER-1, TLA-1, OXY-1–1, XCC-1, KPC-2, BlaC, TEM-76, CTX-M-15, SHV-1, and GES-14 X-ray crystal structures were retrieved from Protein Data Bank, and PDB codes of these enzymes were given in Supplementary file (Table S2). MolProbity is a structure-validation web service that provides an evaluation of model quality for both proteins and nucleic acids. MolProbity scores of 3D protein structure models were varied (Supplementary file Table S3).

And then, all 42 β-lactamases protein structures were verified using the web-based tool ERRAT. If the ERRAT quality factor is 95% and above, the model is in high resolution, and below 91%, the model is in low resolution [22]. Galaxy Web Server [23] was used to minimize the models of β-lactamases.

Molecular docking of three inhibitors to β-lactamases by AutoDock 4.2

After quality checking 42 β-lactamase protein structure models, ligands (relebactam, enmetazobactam, QPX7728) were docked to the active site of the enzymes using AutoDock 4.2 [24]. The active site (T237, T235, S70, K234, S130, K73, and W105) of the KPC-2 enzyme was identified in the study of Hecker et al. [15]. All other enzymes were aligned to KPC-2 using PyMOL, and this active site was used in all docking experiments.

3D structures of relebactam (PubChem CID 44129647), enmetazobactam (PubChem CID 23653540), and QPX7728 (PubChem CID 140830474) were downloaded from PubChem database in SDF format. The file formats of the ligands were converted to the PDBQT format. A complete PDBQT file is partial, and AutoDock must have four atom type information. Hydrogens also must be added to the ligands and the protein. However, non-polar hydrogens were removed, and the binding site was mapped using AutoGrid. For each complex, molecular docking was performed at ten different positions using AutoDock4.2 and the Lamarckian genetic algorithm [25]. A maximum of 25 million energy ratings was applied for each experiment, and the results were clustered using a 2.0-Å tolerance. The 3D structures of the complexes were generated in the PDB format according to their the lowest binding energies.

Molecular dynamics simulations

Inhibitor and protein complexes were simulated by molecular dynamics method for 500 ns. Thus, it was aimed to reveal the molecular basis of the differences in binding affinities. The force fields of atoms were defined AMBER force field (gaff2) and AM1-BCC charge model using the ANTECHAMBER tool in the AMBER package program. The topology and coordinate files of the complexes were generated by adding TIP3PBOX [21] type water in a 10-Å octahedral periodic box using AMBER14 tLEaP [26]. Following, Na + and Cl- were added to neutralize the system. The systems were minimized to remove bad contacts and clashes using 1000-step steepest descent algorithm and 9000-step conjugate algorithm [27–29]. In order to give the first velocity to the molecules, the system [30] was heated to 300 K at constant pressure using Langevin thermostat during 1 ns. As a final step, all complexes were simulated for 500 ns in 2-fs steps at constant temperature, volume, and pressure using the weak coupling temperature algorithm [31].

Results

Amino acid substitutions in the active site of class A β-lactamases

The active site of KPC-2 β-lactamase was shown using PyMOL (Fig. 1). This site is important for binding both substrate and inhibitor. All other 41 β-lactamases active site is the same region with some amino acid substitutions. For in silico studies, β-lactamases with amino acid substitutions in this site were selected, and only one with the same amino acid substitutions was used in molecular docking (Table 1). The phylogenetic tree of class A β-lactamases was shown in Fig. 2.

Quality assessment of 3D protein structure models

Except for two models, the ERRAT quality factor of the other models was above 95%. These two models belong to HER-1 and PAL-1 β-lactamases (Supplementary file Table S2). Galaxy Web Server [23] was used to minimize the models of these β-lactamases. After minimization, the ERRAT quality factor increased to 93.2806% and 92.8571%

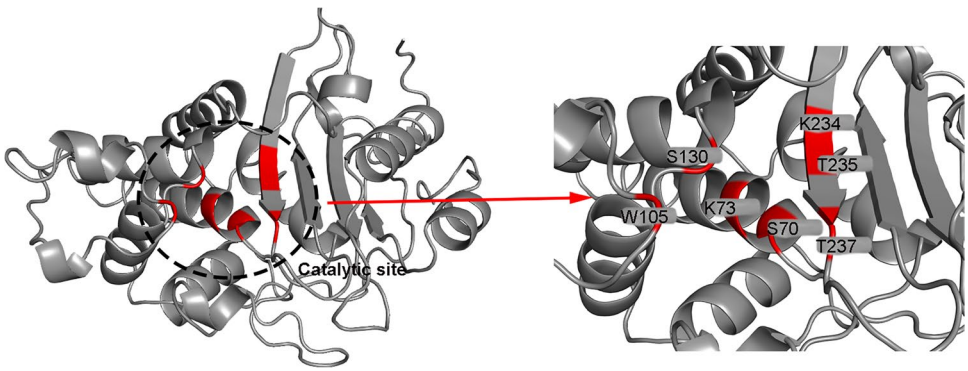

Fig. 1 Amino acid residues in the active site were shown in red (T237, T235, S70, K234, S130, K73, and W105) in KPC-2 β-lactamase

Table 1 Mutations in conserved residues of the active site of β-lactamases

β-Lactamases	Mutations in conserved residues of the active site			
	^{70}SSFK^{73}	W^{105}	^{130}SDN	^{234}K^{235}TG^{237}T
PER (16 allele)	SVFK	W	TDN→PER-4 TDN→PER-14 SDN→ all others	KTGT
TLA (2 allele)	STYK	W	SDN	KTGS
VEB (27 allele)	SVMK	W	TDN→ VEB-24 TDN→ VEB-27 SDN→ all others	RTGT→VEB-20 RTGT→VEB-25 KTGT→ all others
PC-1 (7 allele)	STSK	W→Y	SDN	KSGQ
PC-2 (2 allele)	STLK	W→Y	SDN	KSGQ
HER (7 allele)	STFK	W→Y	SDN	KTGA
CKO (3 allele)	STHK	W→Y	SDN	KTGA
SHV (246 allele)	SAFK→SHV-147 NTFK→ SHV-179 STFK→ all others	W→Y	SDN	RTGA→SHV-56 RTGA→SHV-72 RTGA→ SHV-73 RTGA→ SHV-P11 KTGA→ all others
TEM (243 allele)	STFK	W→N TEM-212 W→F TEM-213 W→S TEM-233 W→Y all others	GDN→ TEM-76 TDN→ S-T TEM 211 TDN→ TEM-224 SDN→ all others	KSGT→TEM-5 KSGT→TEM -24 KSGT→TEM-86 KSGT→ TEM-114 KSGT→TEM-121 KSGT→TEM-130 KSGT→ TEM-131 KSGT→ TEM-136 KSGT→TEM-177 KSGG→TEM-22 KTGA→TEM-230 KSGA→ all others
PAL (8 allele)	STVK	W = = > Y	SDN	RSGA
HMS (2 allele)	STFK	W	SDN	RSGA
GES (48 allele)	STFK	W	CDN→ GES-10 SDN→ all others	KTGA→GES-12 KTGA→GES-33 KTGT→ all others
XCC (24 allele)	STFK	W→H	SDN	KTGS
FRI (10 allele)	SSFK	W→H	SDN	KTGT
IMI (20 allele)	SSFK	W→Y IMI-2 W→N IMI-5 W→H all others	SDN	KTGT→IMI-5 KTGT→IMI-8 KTGS→ all others
KPC (88 allele)	SSFK	W→R KPC-21 W→R KPC-27 W-G→ KPC-22 W→ all others	SDN	KTGT
BlaC	STFK	W→I	SDN	KTGT
CTX-M (251 alleles)	STSK	W→Y	SDH→CTX-M-81 SDH→ CTX-M-181 SDD→ CTX-M 127 SDD→ CTX-M-191 SDD→ CTX-M-215 GDN→ CTX-M-189 GDN→CTX-M-239 TDN→ CTX-M-190 TDN→ CTX-M-199 TDN→ CTX-M-234 TDN→ CTX-M-218	KTGN→CTX-M-103 KTSS→CTX-M-178 KTSS→CTX-M-228 KTGI→CTX-M-100 RTGS→CTX-M-200 RTGS→CTX-M-146 RTGS→ CTX-M-192 RTGS→CTX-M-203 RTGS→ CTX-M-239 RTGS→ CTX-M-P4 RTGS→ CTX-M-P45 KTGS→ all others

Table 1 (continued)

β-Lactamases	Mutations in conserved residues of the active site			
	^{70}SSFK^{73}	W^{105}	^{130}SDN	^{234}K^{235}TG^{237}T
OXY-1(49 alleles)	STSK→ OXY-2–2 STSK→ OXY-2–3 STSK→ OXY-2–4 STSK→ OXY-2–6 STSK→ OXY- 2–7 STSK→ OXY-2–8 STSK→ OXY-2–9 STSK→ OXY-2–17 STSK→ OXY-2–19 STSK→OXY- 2-b STSK→ OXY-2–10 STSK→ OXY-2–11 STSK→ OXY-2–12 STSK→ OXY-2–13 STSK→ OXY-2–14 STSK→ OXY-2–15 STSK→ OXY-2–16 STSK→ OXY-2–18 STSK→ OXY-2–20 STGK→ all others	W	SDN	KTGG→ OXY-1–1 KTGG→ OXY-1–2 KTGG→ OXY-1–3 KTGG→ OXY-1–9 KTGG→ OXY-2–3, KTGG→OXY-2–19 KTGG→ OXY-4–2 KTGG→ OXY-4–3 KTGG→ OXY-4–4 KTGG→ OXY-4–5 KTGT→OXY-2–9 KTGS→OXY-2–14 KTGS→OXY-2-b KTGA→all others
RIC-1 (2 alel)	STSK	W→L RIC-1 W→ RIC-2	SDN	KTGS

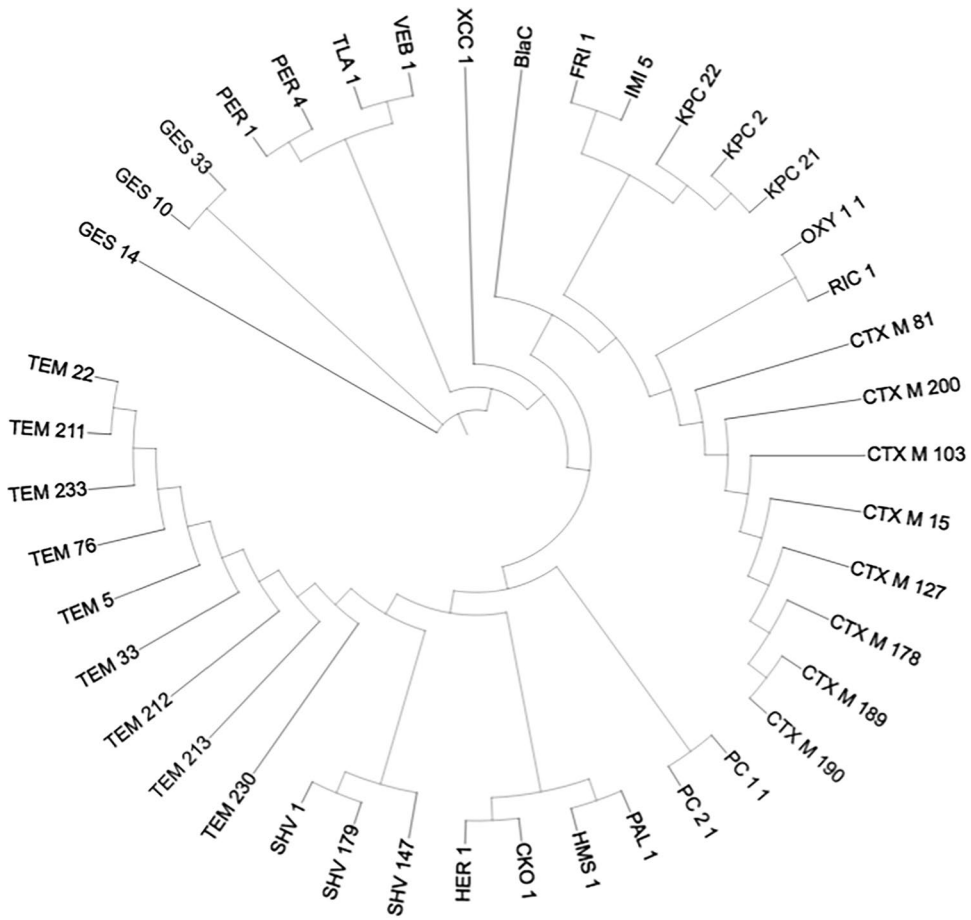

Fig. 2 Phylogenetic tree for 42 class A β-lactamases which were divided into 22 clusters

for HER-1 and PAL-1, respectively. Thus, all models were found to be of adequate quality to be used in molecular docking.

Molecular docking of relebactam, enmetazobactam, and QPX7728 to 42 class A β-lactamases

The lowest binding energies were observed with TEM-76 for relebactam (−7.6 kcal/mol), enmetazobactam (−7.2 kcal/mol), and QPX7728 (−8 kcal/mol). These results indicate a higher binding affinity of these inhibitors to TEM-76 β-lactamase. The β-lactamases with the lowest binding affinity of the inhibitors are CTX-M-81, RIC-1, and CTX-M-200. The lowest and highest binding energies were −7.6 and −4.7 kcal/mol for relebactam, −8 and −4.9 kcal/mol for QPX7728, and −7.2 and −3.9 kcal/mol for enmetazobactam (Supplementary file Table S4).

Compared to other inhibitors (relebactam and QPX7728), it can be said that enmetazobactam has a lower binding affinity for all selected class A β-lactamases. In addition, there were differences between binding energies of inhibitors in allelic variants of some β-lactamases (e.g., CTX-M variants) (Fig. 3).

The binding energies of relebactam, QPX7728, and enmetazobactam to PAL-1 were −7.6, −6.7, and −6.4 kcal/mol, respectively. Among the TEM group β-lactamases (TEM-211, TEM-230, TEM-33, TEM-22, TEM-213, TEM-5, TEM-212, TEM-233), the enzyme with the highest binding affinity of the inhibitors was TEM-76. The inhibitor with the lowest binding energy for TLA-1 and CKO-1 was relebactam (−6.5 kcal/mol and −5.8 kcal/mol). Allelic mutations of GES-14 and GES-33 did not significantly change the binding energies of the three inhibitors. However, relebactam and QPX7728 had higher binding energy for GES-10 type β-lactamase compared to GES-14 and GES-33. QPX7728 had higher binding energy for VEB-1 than enmetazobactam and relebactam (−6.5 kcal/mol). Allelic mutation between PER-1 and PER-4 did not cause a significant change in binding energies of inhibitors. Relebactam binding energy for CTX-M-81 was higher in comparison to other CTX-M-type β-lactamases (CTX-M-200, CTX-M-190, CTX-M-15, CTX-M-178, CTX-M-127, CTX -M-189, CTX-M-103). Besides, the binding energies of QPX7728 against CTX-M variants were similar. Among the CTX-M variants, enmetazobactam bound to CTX-M-15 with the lowest binding energy (−5.4 kcal/mol), while CTX-M-200 with the highest binding energy (−3.9 kcal/mol). Among the three inhibitors for PC-2–1 and PC-1–1, relebactam and QPX7728 had low binding energy, and mutations between these two enzymes had no significant effect on binding energies. While enmetazobactam bound to SHV variants (SHV-1, SHV-179, and SHV-147) with a higher binding affinity than other inhibitors, similar binding energies of QPX7728 and relebactam for SHV-1, SHV-179, and SHV-147 were observed. The binding energies of relebactam, QPX7728, and enmetazobactam for OXY-1–1 are −6 kcal/mol, −6.7 kcal/mol, and −5.6 kcal/mol, respectively. The binding energies of QPX7728 and enmetazobactam were similar for HER-1 and HMS-1. The binding energies of relebactam for HMS-1 and HER-1 were −6.1 kcal/mol and −7.1 kcal/mol, respectively.

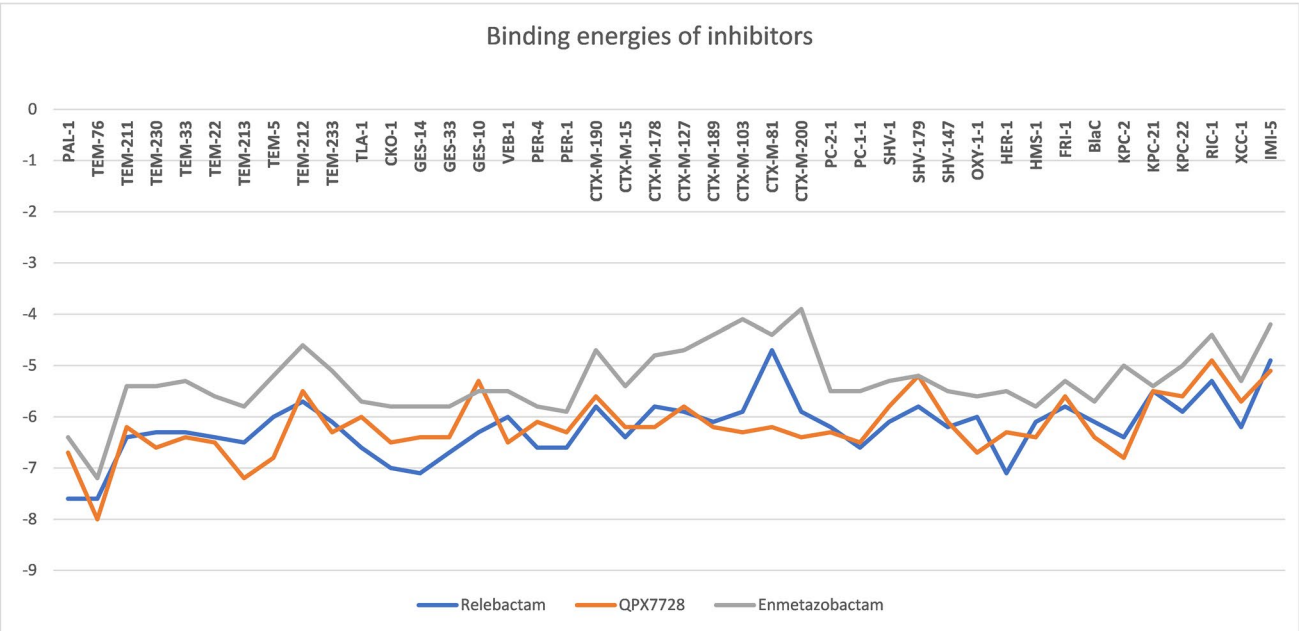

Fig. 3 Binding energy changes of relebactam, QPX7728, and enmetazobactam to all class A β-lactamases

Relebactam, QPX7728, and enmetazobactam binding energies against BlaC were close to each other. The inhibitor with the highest binding affinity for KPC-2 was QPX7728. However, the binding affinity of this inhibitor was decreased in KPC-21 and KPC-22 variants. Relebactam had the lowest binding energy for RIC-1 when compared to other inhibitors. The binding energies of the three inhibitors were similar for XCC-1 and − 6.2 kcal/mol for relebactam, − 5.7 kcal/mol for QPX7728, and − 5.3 kcal/mol for enmetazobactam. All three inhibitors had a low binding affinity against IMI-5 (Table 2).

Molecular dynamic simulation

The selected β-lactamase–substrate complexes, TEM-76-relebactam, CTX-M-81-relebactam, TEM-76-enmetazobactam, and CTX-M-200-enmetazobactam, were simulated 500 ns. Fluctuations of enzymes and stability of relebactam and enmetazobactam were analyzed. First of all, a root mean square graph was drawn to analyze whether the complexes reached thermodynamic equilibrium during 500 ns MD. In the graph drawn based on the α-carbons of enzymes, all complexes reached equilibrium around 70–80 ns (Fig. 4).

The fluctuations of the residues in the enzyme during the 500-ns MD simulation were demonstrated by plotting the B-factor graph. The B-factor is known as the temperature factor and is directly related to the root mean square fluctuation. The B factor is formulated with $B = 8/3\pi^2 \times u^2$ and represents the average displacement with the unit u Å in the equation. Regions with low B-factor values are constant, while high ones represent flexible regions. In the complexes, B-factor plots, the feature Ω-loop region showed the greatest fluctuation. The other two regions (sites 1 and 2) that show high fluctuation were the regions around the substrate binding region (Fig. 5).

In order to follow the mobility of the substrates, the variation of the distance between the catalytic residue serine and the substrates was analyzed during 500 ns (Fig. 6).

After simulation, the interactions of relebactam and enmetazobactam were described by a residual 2-dimensional interaction diagram (Fig. 7).

Discussion

Relebactam, which has the potential to inhibit class A and C β-lactamases, is effective to reverse imipenem resistance in imipenem-resistant *Enterobacteriaceae* and *Pseudomonas aeruginosa* when used in combination with imipenem [32]. β-Lactamase inhibition mechanism of relebactam occurs by covalent binding of the inhibitor's opened ring to the active site serine, and this mechanism also applies to other DBOs (diazabicyclooctanes). The new boronic acid-based inhibitor is QPX7728, and it can inhibit enzymes such as KPC, NDM, VIM, and OXA-48, which cause resistance in carbapenem-resistant *Acinetobacter baumannii* and *Enterobacteriaceae*. QPX7728 has a compact structure and can fit into the active site. It does not have side chains to interact with distant sites,

Table 2 The estimated free binding energies of relebactam, enmetazobactam, and QPX7728

β-lactamases	The estimated free binding energy (kcal/mol)		
	Relebactam	QPX7728	Enmetazobactam
PAL-1	− 7.6	− 6.7	− 6.4
TEM-76	− 7.6	− 8	− 7.2
TEM-211	− 6.4	− 6.2	− 5.4
TEM-230	− 6.3	− 6.6	− 5.4
TEM-33	− 6.3	− 6.4	− 5.3
TEM-22	− 6.4	− 6.5	− 5.6
TEM-213	− 6.5	− 7.2	− 5.8
TEM-5	− 6	− 6.8	− 5.2
TEM-212	− 5.7	− 5.5	− 4.6
TEM-233	− 6.1	− 6.3	− 5.1
TLA-1	− 6.6	− 6	− 5.7
CKO-1	− 7	− 6.5	-5.8
GES-14	− 7.1	-6.4	− 5.8
GES-33	− 6.7	-6.4	− 5.8
GES-10	− 6.3	− 5.3	− 5.5
VEB-1	− 6	− 6.5	− 5.5
PER-4	− 6.6	− 6.1	− 5.8
PER-1	− 6.6	− 6.3	− 5.9
CTX-M-190	− 5.8	− 5.6	− 4.7
CTX-M-15	− 6.4	− 6.2	− 5.4
CTX-M-178	− 5.8	− 6.2	− 4.8
CTX-M-127	− 5.9	− 5.8	− 4.7
CTX-M-189	− 6.1	− 6.2	− 4.4
CTX-M-103	− 5.9	− 6.3	− 4.1
CTX-M-81	− 4.7	− 6.2	− 4.4
CTX-M-200	− 5.9	− 6.4	− 3.9
PC-2–1	− 6.2	− 6.3	− 5.5
PC-1–1	− 6.6	− 6.5	− 5.5
SHV-1	− 6.1	− 5.8	− 5.3
SHV-179	− 5.8	− 5.2	− 5.2
SHV-147	− 6.2	− 6.1	− 5.5
OXY-1–1	− 6	− 6.7	− 5.6
HER-1	− 7.1	− 6.3	− 5.5
HMS-1	− 6.1	− 6.4	− 5.8
FRI-1	− 5.8	− 5.6	− 5.3
BlaC	− 6.1	− 6.4	− 5.7
KPC-2	− 6.4	− 6.8	− 5
KPC-21	− 5.5	− 5.5	− 5.4
KPC-22	− 5.9	− 5.6	− 5
RIC-1	− 5.3	− 4.9	− 4.4
XCC-1	− 6.2	− 5.7	− 5.3
IMI-5	− 4.9	− 5.1	− 4.2

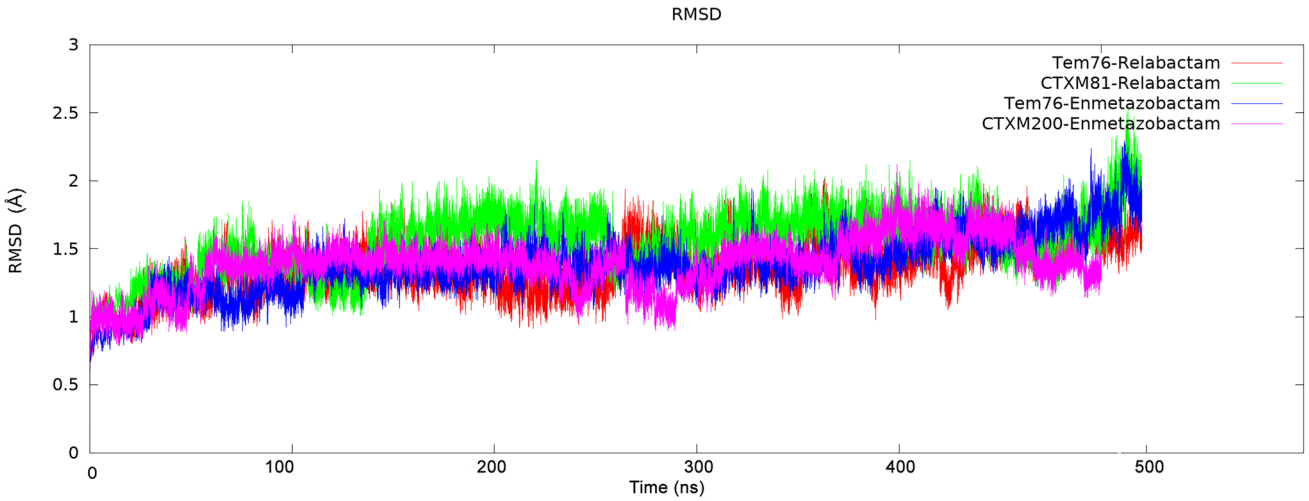

Fig. 4 Root mean square deviation of enzyme based on α-carbon during 500-ns MD simulation. TEM-76-relebactam, CTX-M-81-relebactam, TEM-76-enmetazobactam, and CTX-M-200-enmetazobactam were shown in red, green, blue, and pink line, respectively

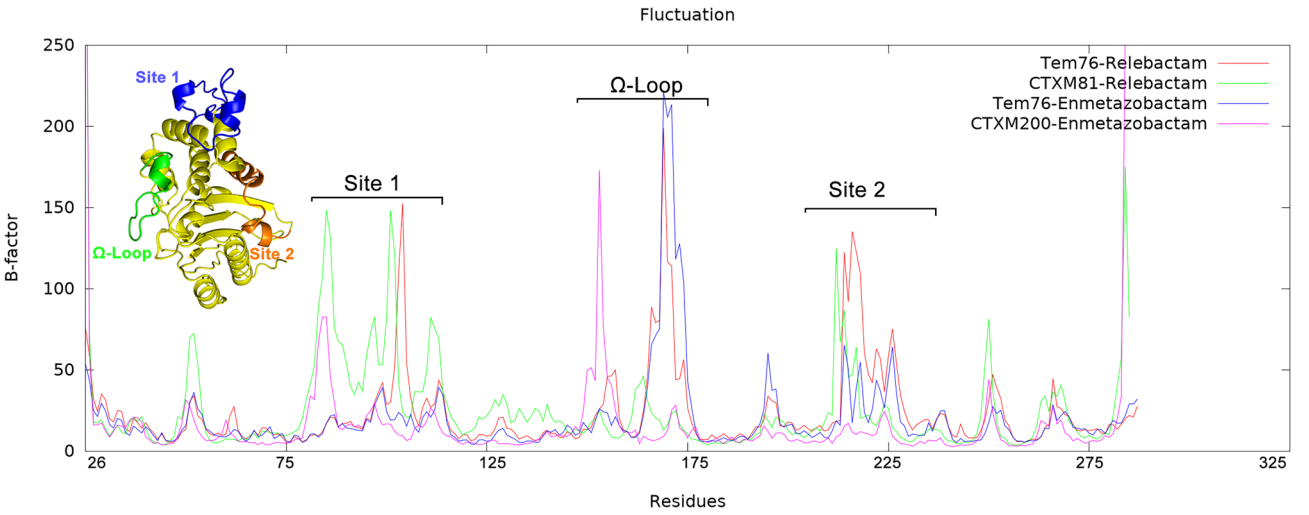

Fig. 5 The fluctuation of residues based on α-carbon during 500 ns MD simulation. TEM-76-relebactam, CTX-M-81-relebactam, TEM-76-enmetazobactam, and CTX-M-200-enmetazobactam were shown in red, green, blue, and pink line, respectively

which may leave it unaffected by mutational changes in β-lactamases. Boronic acid-based inhibitors perform inhibition by the mechanism based on the formation of a covalent bond between boronate with the active site serine and the formation of a tetrahedral intermediate, which is a transition state analog [11]. Enmetazobactam, which shares a similar structure with tazobactam, has a methyl group on its triazole moiety and inhibits class A β-lactamases, including KPC [12]. In different studies, the IC50 values of relebactam, QPX7728, and enmetazobactam for KPC carbapenemase were found to be 82 nm, 2.9 nm, and ≤ 0.52 μM, respectively [11, 12]. As it is known, the formation of different types in class A β-lactamases and also new alleles with mutations within these types has been increased rapidly. Of class A β-lactamases, only the CTX-M-type β-lactamase has 251 alleles. If we talk about β-lactamase types, there are about 116 different types of class A β-lactamases.

In the current study, β-lactamases and their allelic variations in terms of mutations in active site residues were screened. In silico methods were used for revealing how relebactam, QPX7728, and enmetazobactam would be affected by these mutational changes by selecting 42 class A β-lactamases with active residue substitutions. The effect of mutational changes on binding energies within all class A β-lactamases may be relevant to design of inhibitors. In the first part of the study, relebactam, enmetazobactam,

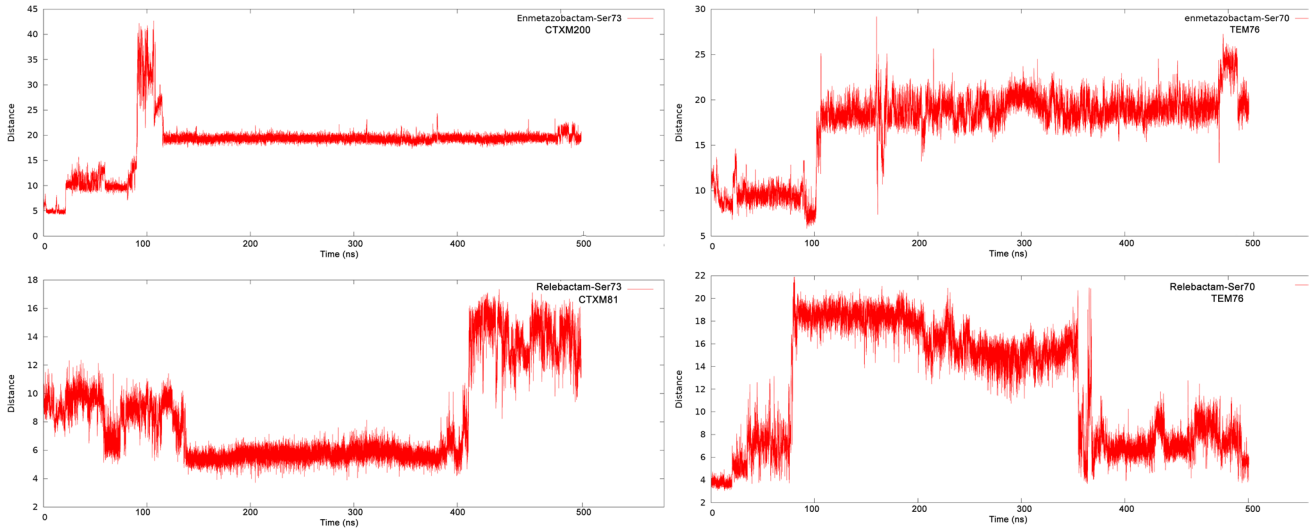

Fig. 6 The distance (Å) of between substrate and catalytic residue S70 α-carbon during 500-ns MD simulation

and QPX7728 were docked to the active site of 42 class A β-lactamases by molecular docking method, and estimated free binding energies (kcal/mol) were calculated with AutoDock 4.2.

PER-4 has an S→T substitution at position 130 (compared to PER-1), and this substitution did not cause a significant change in the binding energies of the three inhibitors. It was determined that the S130T mutation did not cause a conformational change in CTX-M type β-lactamases but only when sulbactam was bound, a conformational change that weakened the binding of sulbactam occurred [33]. It can be speculated from our results that the S130T mutation did not result in a conformational change that would alter the binding affinity of relebactam, QPX7728, and enmetazobactam to PER-type β-lactamases. However, in a study evaluating the effect of Ω-loop variations on avibactam inhibition, S130T variants were found to be resistant to MIC alterations by avibactam [34]. These studies showed that the effect of mutations in β-lactamases was variable according to the inhibitor. S70N and S71A mutations in SHV-type β-lactamases caused a slightly increase in the binding energy of QPX7728 (Table 2). The binding energy of QPX7728 to SHV-1 was − 5.8 kcal/mol, while the binding energies of SHV-179 and SHV-147 were − 5.2 and − 6.1, respectively. Interestingly, significant changes in binding energies of QPX7728, relebactam, and enmetazobactam were seen for TEM variants. TEM-33 had S70, Y105, S130, K234, S235, and A237 in its active site. For the three inhibitors, binding energies against TEM-212 (Y105N) were slightly decreased compared to TEM-33. Compared to TEM-33, the S130G (TEM-76) mutation reduced the binding energies of QPX7728, relebactam, and enmetazobactam, whereas the S130T mutation had no significant effect on the binding energies of these three inhibitors for TEM-211. From this, it was assumed that the S130T mutation did not have a significant effect on the binding energies of inhibitors for TEM-type and PER-type β-lactamases. When compared to TEM-33, A237T (TEM-5) and A237G (TEM-22) mutations did not affect significantly the binding energies of inhibitors. When the GES-10 (S130C) and GES-33 (T237A) variants were compared with GES-14, the binding affinity of relebactam and QPX7728 was decreased. The binding energies of QPX7728 to KPC-21 and KPC-22 were increased, which was due to the mutations of W105R (KPC-21) and W105G (KPC-22) found in these variants as compared to KPC-2. Among the CTX-M variants, significant differences were observed in the binding energies of enmetazobactam and relebactam. The binding energies of enmetazobactam for CTX-M-15 and CTX-M-200 (K234R) were 5.4 kcal/mol and − 3.9 kcal/mol, respectively. Also, the binding energy of relebactam for CTX-M-15 was − 6.4 kcal/mol and for CTX-M-81 was − 4.7 kcal/mol. K234R substitution in the inhibitor-resistant CTX-M β-lactamase variant causes an increasing resistance to clavulanic acid which has been determined in previous studies [35]. In terms of binding affinities of three inhibitors, CTX-M β-lactamases carrying the K234R mutation were more resistant to enmetazobactam than others. Relebactam has piperidine in its R1-side chain [36]. The 2D representation of interactions between ligands and β-lactamases before MD simulation showed that N-atom of piperidine did hydrogen bond with THR219 in CTX-M-81-relebactam complex but with SER235 in TEM-76-relebactam complex (Figure S3). SER235 residue of TEM-type β-lactamases makes hydrogen bonds with the substrates and is important in catalytic activity [37]. Enmetazobactam has inhibitory activity toward CTX-M, TEM, SHV, and other

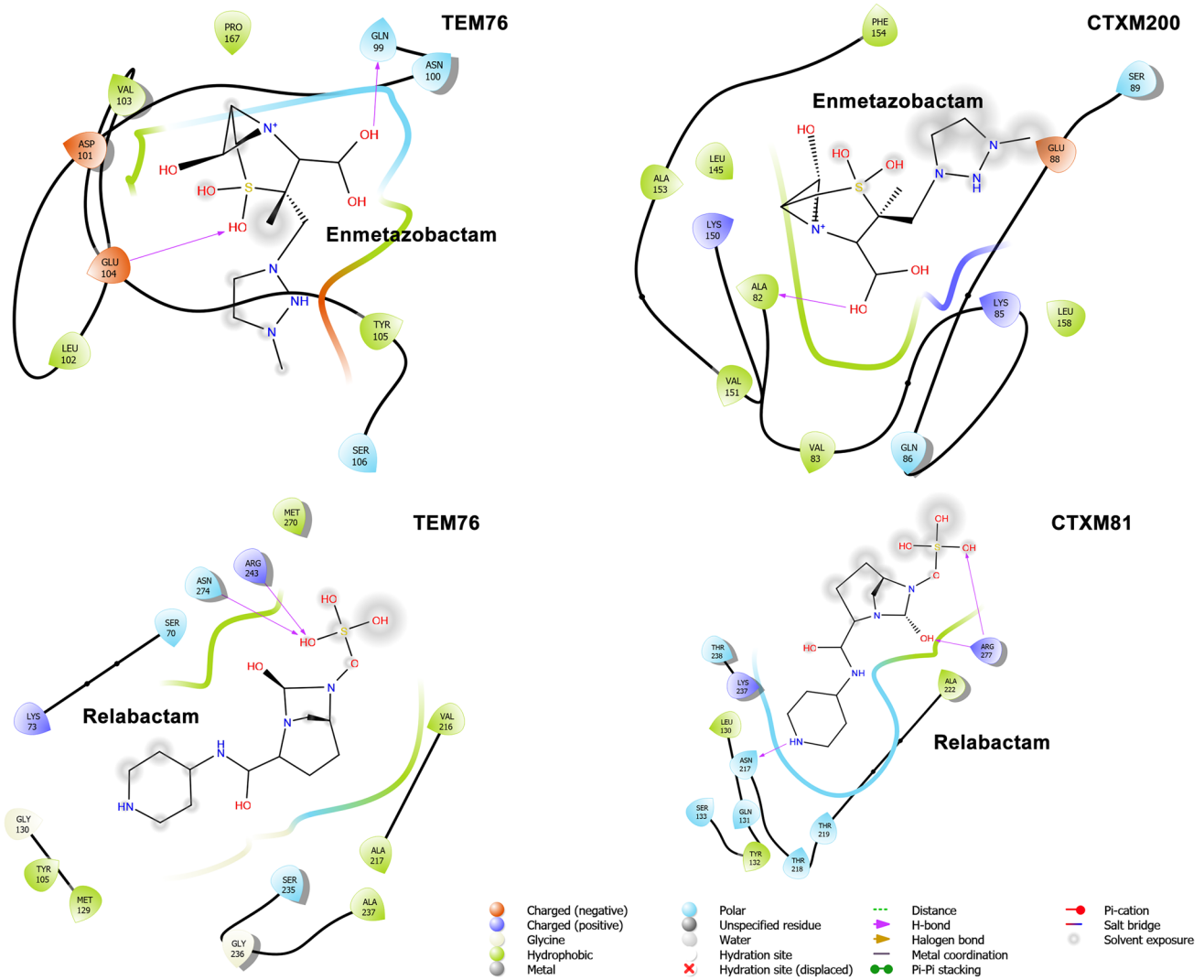

Fig. 7 A 2D representation of the interaction between enzyme and substrate after 500-ns MD simulation. All markers and ligand interaction diagram legends were shown below the figure

class A β-lactamases [38, 39]. There was no hydrogen bond between enmetazobactam and CTX-M-200 according to 2D representation. On the other hand, enmetazobactam made hydrogen bond with S235 in TEM-76-enmetazobactam complex (Figure S3). According to our results, hydrogen bond at position 235 of TEM-76 was important for the first docking to enzyme.

The selected β-lactamase-substrate complexes TEM-76-relebactam, CTX-M-81-relebactam, TEM-76-enmetazobactam, and CTX-M-200-enmetazobactam were simulated 500 ns. In the graph drawn based on the α-carbons of enzymes, all complexes reached equilibrium around 70–80 ns (Fig. 4). If the complexes were simulated as short as 100 ns, it could be said that all substrates remained stable in the structure. In further analysis, 3-dimensional structures of the complexes were created at 20-ns intervals throughout the simulation (movie was not supplemented). In these complexes, it was observed that enmetazobactam did not remain stable in the cavity where it was bound and was bound to another site after association. On the other hand, relebactam remained stable in TEM-76, but not in CTX-M-81, which gave lower docking binding affinity. When analyzed throughout the simulation, relebactam was gone away from its binding cavity and rebinding (Figure S4). These associate and disassociate caused partial changes in the RMSD values of the enzymes. When the 3-dimensional structure of the enzymes was examined, it was seen that there were no significant changes in the secondary and tertiary structures and the 500-ns-long MD simulation was sufficient for the analysis of the interactions. The fluctuations of the residues in the enzyme during the 500-ns MD simulation were demonstrated by plotting the B-factor graph. According to the

results of docking to TEM-76 enzyme, higher atomic substitution occurred in relebactam and enmetazobactam complexes with high binding affinity. While these substrates were more stable in the binding cavity of the TEM-76 enzyme, the binding was weaker in the CTX-M group enzymes, and therefore the Ω-loop region remained more stable. Another striking difference was the high volatility between 150 and 160th residues of the CTX-M-200-enmetazobactam complex (Fig. 5). Considering the 3-dimensional structure, after enmetazobactam left the active cavity, it was bound between the α-helix structure formed by 150th and 160th residues and remained stable in this region for 500 ns. In order to follow the mobility of the ligands, the variation of the distance between the serine, the catalytic residue in the enzymes, and the substrates during 500 ns was analyzed. While the distance between S73 α-carbon in the active site of CTX-M-200 and enmetazobactam was around 6 Å, enmetazobactam remained stable between the α-helix structure after disassociation during the simulation and did not change position for 500 ns (Fig. 4). While the distance between enmetazobactam and TEM-76 S70 α-carbon was 9 Å, it was located at a distance of 20 Å after about 100 ns and remained constant here. This region is a loop located between residues 99–110 at the top of the active region (Fig. 6). On the other hand, while the distance between CTX-M-81 S73 α-carbon was around 10 Å, relebactam approached 5 Å around 150 ns and remained stable up to 400 ns. Looking at the distance graph, relebactam moved away from the region and remained stable at a distance of 14 Å. In TEM76, while it was 5 Å away, after 100 ns, the distance remained stable for 250 ns at 18 Å away. However, when the 3-dimensional structure formed every 20 ns was analyzed (figure not shown), it was seen that Relebactam was in the binding cavity, but the inhibitor only tumbled according to its initial position. It was observed that the last 150-ns relebactam returned to its starting position and remained stable at 6 Å away (Fig. 6). This shows that relebactam remains stable closer to S70 [40], which is important in catalytic activity. After simulation, relebactam and enmetazobactam and their interactions with residues were described by a 2-dimensional interaction diagram (Fig. 7). Enmetazobactam made hydrogen bonds with polar residue Gln99 and negatively charged residue Glu104 of TEM-76. This interaction was seen in a loop located between residues 99–110 at the top of the binding site. In CTX-M-200, it was seen that enmetazobactam was located completely outside the binding cavity. Enmetazobactam made hydrogen bond with the hydrophobic residue of Ala82 (Fig. 7). Relebactam was more stable than enmetazobactam and hydrogen bonded with polar residue Asn274 and positive residue Arg243 in the binding cavity of TEM-76. In the binding cavity of CTX-M-81, it made three hydrogen bonds, one with the polar residue Asn217 and two with the positive residue Arg277 (Fig. 7).

In conclusion, molecular docking results showed that relebactam and QPX7728 were more favorable inhibitors for 42 class A β-lactamases. Inhibitors had slightly different binding affinities in variants of class A β-lactamases. The enzyme with the highest binding affinities for enmetazobactam and relebactam was an inhibitor-resistant TEM-76 β-lactamase. The 2D representation of interactions after molecular docking showed that TEM-76 made hydrogen bonds with S235. This may enable us to speculate that this residue is a position to be considered in inhibitor design. The enzymes to which relebactam and enmetazobactam bound with the lowest and highest binding affinities were selected and the underlying mechanism in differentiation between binding energies were aimed to be revealed by molecular dynamic simulation. As a result of the analyzes made after the molecular dynamics simulation carried out for 500 ns, it was concluded that the distance from S70, stability in the enzyme active cavity, and high atomic displacement would be the factors affecting the binding affinity of inhibitors to class A β-lactamases.

Supplementary Information The online version contains supplementary material available at https://doi.org/10.1007/s00894-022-05073-3.

Acknowledgements Numerical calculations including MD simulations were carried out at TUBITAK ULAKBIM (TURKEY), High Performance and Grid Computing Center (TRUBA).

Author contribution Ayşegül Saral Sarıyer contributed to the design and implementation of the research, to the analysis of the results, and to the writing of the manuscript.

Availability of data and material Not applicable.

Code availability Not applicable.

Declarations

Conflicts of interest The authors declare no competing interests.

References

1. Bush K (2010) Bench-to-bedside review: the role of β-lactamases in antibiotic-resistant Gram-negative infections. Crit Care 14:224. https://doi.org/10.1186/cc8892
2. Silveira MC, Azevedo R, da Silva F, Faria da Mota M, Jardim Catanho R, Guimarães ACR, de Miranda AB (2018) Systematic identification and classification of β-lactamases based on sequence similarity criteria: β-lactamase annotation. Evol Bioinform 10(14):1176934318797351. https://doi.org/10.1177/1176934318797351
3. Bonomo RA (2017) β-lactamases: a focus on current challenges. Cold Spring Harb Perspect Med 7(1):a025239. https://doi.org/10.1101/cshperspect.a025239
4. Ambler RP (1908) The structure of beta-lactamases. Philos Trans R Soc B Biol Sci 289(1036):321–331. https://doi.org/10.1098/rstb.1980.0049

5. Philippon A, Jacquier H, Ruppé E, Labia R (2019) Structure-based classification of class A beta-lactamases, an update. Curr Res Transl Med 67(4):115–122. https://doi.org/10.1016/j.retram.2019.05.003
6. Khanna NR, Gerriets V. Beta lactamase inhibitors. In: StatPearls. StatPearls Publishing, Treasure Island. https://www.ncbi.nlm.nih.gov/books/NBK557592/. Accessed 1 Sept 2021
7. Tooke CL, Hinchliffe P, Bragginton EC, Colenso CK, Hirvonen VHA, Takebayashi Y, Spencer J (2019) β-lactamases and β-lactamase inhibitors in the 21st century. J Mol Biol 431:3472–3500. https://doi.org/10.1016/j.jmb.2019.04.002
8. Shapiro AB, Gao N (2021) Interactions of the diazabicyclooctane serine β-lactamase inhibitor ETX1317 with target enzymes. ACS Infect Dis 7(1):114–122. https://doi.org/10.1021/acsinfecdis.0c00656
9. Vázquez-Ucha JC, Arca-Suárez J, Bou G, Beceiro A (2020) New carbapenemase inhibitors: clearing the way for the β-lactams. Int J Mol Sci 21(23):9308. https://doi.org/10.3390/ijms21239308
10. Krajnc A, Brem J, Hinchliffe P, Calvopiña K, Panduwawala TD, Lang PA, Kamps J, Tyrrell JM, Widlake E, Saward BG, Walsh TR, Spencer J, Schofield CJ (2019) Bicyclic boronate VNRX-5133 inhibits metallo- and serine-β-lactamases. J Med Chem 62(18):8544–8556. https://doi.org/10.1021/acs.jmedchem.9b00911
11. Tsivkovski R, Totrov M, Lomovskaya O (2020) Biochemical characterization of QPX7728, a new ultrabroad-spectrum beta-lactamase inhibitor of serine and metallo-beta-lactamases. Antimicrob Agents Chemother 64(6):e00130-e220. https://doi.org/10.1128/AAC.00130-20
12. Papp-Wallace KM (2019) The latest advances in β-lactam/β-lactamase inhibitor combinations for the treatment of Gram-negative bacterial infections. Expert Opin Pharmacother 20(17):2169–2184. https://doi.org/10.1080/14656566.2019.1660772
13. Russ D, Glaser F, Shaer Tamar E, Yelin I, Baym M, Kelsic ED, Zampaloni C, Haldimann A, Kishony R (2020) Escape mutations circumvent a tradeoff between resistance to a beta-lactam and resistance to a beta-lactamase inhibitor. Nat Commun 11(1):2029. https://doi.org/10.1038/s41467-020-15666-2
14. Tooke CL, Hinchliffe P, Lang PA, Mulholland AJ, Brem J, Schofield CJ, Spencer J (2019) Molecular basis of class a β-lactamase inhibition by relebactam. Antimicrob Agents Chemother 63(10):e00564-e619. https://doi.org/10.1128/AAC.00564-19)
15. Hecker SJ, Reddy KR, Lomovskaya O, Griffith DC, Rubio-Aparicio D, Nelson K, Tsivkovski R, Sun D, Sabet M, Tarazi Z, Parkinson J, Totrov M, Boyer SH, Glinka TW, Pemberton OA, Chen Y, Dudley MN (2020) Discovery of cyclic boronic acid QPX7728, an ultrabroad-spectrum inhibitor of serine and metallo-β-lactamases. J Med Chem 63(14):7491–7507. https://doi.org/10.1021/acs.jmedchem.9b01976
16. Meng Y, Zhang HX, Mezei M, Cui M (2011) Molecular docking: a powerful approach for structure-based drug discovery. Curr Comput Aided Drug Des 7(2):146–157. https://doi.org/10.2174/157340911795677602
17. Hollingsworth SA, Dror RO (2018) Molecular dynamics simulation for All. Neuron 99(6):1129–1143. https://doi.org/10.1016/j.neuron.2018.08.011
18. Naas T, Oueslati S, Bonnin RA, Dabos ML, Zavala A, Dortet L, Retailleau P, Iorga BI (2017) Beta-lactamase DataBase (BLDB)-struct function. J Enzyme Inhib Med Chem 32:917–919. https://doi.org/10.1080/14756366.2017.1344235
19. Steinegger M, Söding J (2017) MMseqs2 enables sensitive protein sequence searching for the analysis of massive data sets. Nat Biotechnol 35(11):1026–1028. https://doi.org/10.1038/nbt.3988
20. Lefort V, Desper R, Gascuel O, FastME 2.0 (2015) A comprehensive, accurate, and fast distance-based phylogeny inference program. Mol Biol Evol 32(10):2798–2800. https://doi.org/10.1093/molbev/msv150
21. Waterhouse A, Bertoni M, Bienert S, Studer G, Tauriello G, Gumienny R, Heer FT, de Beer TAP, Rempfer C, Bordoli L, Lepore R, Schwede T (2018) SWISS-MODEL: homology modelling of protein structures and complexes. Nucleic Acids Res 46(W1):W296–W303. https://doi.org/10.1093/nar/gky427
22. Colovos C, Yeates TO (1993) Verification of protein structures: patterns of nonbonded atomic interactions. Protein Sci 2(9):1511–1519. https://doi.org/10.1002/pro.5560020916
23. Ko J, Park H, Heo L, Seok C (2012) GalaxyWEB server for protein structure prediction and refinement. Nucleic Acids Res 40(W1):W294–W297. https://doi.org/10.1093/nar/gks493
24. Forli W, Halliday S, Belew R, Olson AJ (2012) AutoDock Version 4.2. J Med Chem 55:623–638. https://doi.org/10.1021/jm2005145
25. Morris GM, Goodsell DS, Halliday RS, Huey R, Hart WE, Belew RK, Olson AJ (1998) Automated docking using a Lamarckian genetic algorithm and an empirical binding free energy function. J Comput Chem 19:1639–1662
26. Case DA et al (2012) AMBER 12. University of California, San Francisco
27. Jorgensen WL, Chandrasekhar J, Madura JD (1983) Comparison of simple potential functions for simulating liquid water. J Chem Phys 79:926. https://doi.org/10.1063/1.445869
28. Fletcher R, Powell MJD (1963) A rapidly convergent descent method for minimization. Comput J 6(2):163–168. https://doi.org/10.1093/COMJNL/6.2.163
29. Fletcher R, Reeves CM (1964) Function minimization by conjugate gradients. Comput J 7(2):149–154. https://doi.org/10.1093/comjnl/7.2.149
30. Pastor W, Brooks BR, Szabo A (1988) An analysis of the accuracy of Langevin and molecular dynamics algorithms. Mol Phys 65(6):1409–1419. https://doi.org/10.1080/00268978800101881
31. Berendsen HJC, Postma JPM, van Gunsteren WF, DiNola A, Haak JR (1984) Molecular dynamics with coupling to an external bath. J Chem Phys 81:3684. https://doi.org/10.1063/1.448118
32. Smith JR, Rybak JM, Claeys KC (2020) Imipenem-cilastatin-relebactam: a novel β-lactam-β-lactamase inhibitor combination for the treatment of multidrug-resistant gram-negative infections. Pharmacotheraphy 40(4):343–356. https://doi.org/10.1002/phar.2378
33. Cheng Q, Xu C, Chai J, Zhang R, Wai Chi Chan E, Chen S (2020) Structural insight into the mechanism of inhibitor resistance in CTX-M-199, a CTX-M-64 variant carrying the $S^{130}T$ substitution. ACS Infect Dis 6(4):577–587. https://doi.org/10.1021/acsinfecdis.9b00345
34. Lahiri SD, Bradford PA, Nichols WW, Alm RA (2016) Structural and sequence analysis of class A β-lactamases with respect to avibactam inhibition: impact of Ω-loop variation. J Antimicrob Chemother 71(10):2848–2855. https://doi.org/10.1093/jac/dkw248
35. Soeung V, Lu S, Hu L, Judge A, Sankaran B, Prasad BVV, Palzkill T (2020) A drug-resistant β-lactamase variant changes the conformation of its active-site proton shuttle to alter substrate specificity and inhibitor potency. J Biol Chem 295(52):18239–18255. https://doi.org/10.1074/jbc.RA120.016103
36. Zhanel GG, Lawrence CK, Adam H, Schweizer F, Zelenitsky S, Zhanel M, Lagacé-Wiens PRS, Walkty A, Denisuik A, Golden A, Gin AS, Hoban DJ, Lynch JP, Karlowsky JA (2018) Imipenem-relebactam and meropenem-Vaborbactam: Two novel carbapenem-β-lactamase inhibitor combinations. Drugs 78(1):65–98. https://doi.org/10.1007/s40265-017-0851-9
37. Imtiaz U, Manavathu EK, Lerner SA, Mobashery S (1993) Critical hydrogen bonding by serine 235 for cephalosporinase activity of TEM-1 beta-lactamase. Antimicrob Agents Chemother 37(11):2438–2442. https://doi.org/10.1128/aac.37.11.2438

38 Morrissey I, Magnet S, Hawser S, Shapiro S, Knechtle P (2019) *In vitro* activity of cefepime-enmetazobactam against gram-negative isolates collected from U.S. And European hospitals during 2014–2015. Antimicrob Agents Chemother 63(7):e00514-19. https://doi.org/10.1128/AAC.00514-19

39. Papp-Wallace KM, Bethel CR, Caillon J, Barnes MD, Potel G, Bajaksouzian S, Rutter JD, Reghal A, Shapiro S, Taracila MA, Jacobs MR, Bonomo RA, Jacqueline C (2019) Beyond piperacillin-tazobactam: cefepime and AAI101 as a potent β-lactam-β-lactamase inhibitor combination. Antimicrob Agents Chemother 63(5):e00105-e119. https://doi.org/10.1128/AAC.00105-19

40. He Y, Lei J, Pan X, Huang X, Zhao Y (2020) The hydrolytic water molecule of class a β-lactamase relies on the acyl-enzyme intermediate ES* for proper coordination and catalysis. Sci Rep 10:10205. https://doi.org/10.1038/s41598-020-66431-w

Publisher's note Springer Nature remains neutral with regard to jurisdictional claims in published maps and institutional affiliations.